International Journal of Nanomedicine

Dovepress

open access to scientific and medical research

Open Access Full Text Article

ORIGINAL RESEARCH

An MRI-visible non-viral vector for targeted Bcl-2 siRNA delivery to neuroblastoma

This article was published in the following Dove Press journal:
International Journal of Nanomedicine
29 June 2012
Number of times this article has been viewed

Min Shen[1,*]
Faming Gong[3,*]
Pengfei Pang[1,*]
Kangshun Zhu[1]
Xiaochun Meng[1]
Chun Wu[1]
Jin Wang[1]
Hong Shan[1,2]
Xintao Shuai[3,4]

[1]Molecular Imaging Lab, Department of Radiology, The Third Affiliated Hospital of Sun Yat-sen University, Guangzhou, China; [2]Institute of Intervention Radiology, Sun Yat-sen University, Guangzhou, China; [3]PCFM Lab of Ministry of Education, School of Chemistry and Chemical Engineering, Sun Yat-sen University, Guangzhou, China; [4]Center of Biomedical Engineering, Zhongshan School of Medicine, Sun Yat-Sen University, Guangzhou, China

*These authors contributed equally to this work

Correspondence: Hong Shan
Molecular Imaging Lab, Department of Radiology, The Third Affiliated Hospital of Sun Yat-sen University, Guangzhou 510630, China
Tel +86 208 525 2316
Fax +86 208 525 2606
Email shanhong@mail.sysu.edu.cn

Xintao Shuai
PCFM Lab of Ministry of Education, School of Chemistry and Chemical Engineering, Sun Yat-sen University, Guangzhou 510275, China
Tel +86 208 411 2105
Fax +86 208 411 2245
Email shuaixt@mail.sysu.edu.cn

Abstract: Polyethylene glycol-grafted polyethylenimine (PEG-g-PEI) which was functionalized with a neuroblastoma cell-specific ligand, the GD2 single chain antibody ($scAb_{GD2}$), was synthesized in order to effectively deliver Bcl-2 siRNA into neuroblastoma cells. This polymer was complexed first with superparamagnetic iron oxide nanoparticle (SPION) to get a MRI-visible targeted non-viral vector ($scAb_{GD2}$-PEG-g-PEI-SPION) and then with Bcl-2 siRNA to form nanoparticles showing low cytotoxicity. The targeting capacity of $scAb_{GD2}$-PEG-g-PEI-SPION was successfully verified in vivo and in vitro by magnetic resonance imaging. The single chain antibody encoded targeted polyplex was more effective in transferring Bcl-2 siRNA than the nontargeting one in SK-N-SH cells, a human neuroblastoma cell line, resulting in a 46.34% inhibition in the expression of Bcl-2 mRNA. Consequently, a high level of cell apoptosis up to 50.76% and a significant suppression of tumor growth were achieved, which indicates that $scAb_{GD2}$-PEG-g-PEI-SPION is a promising magnetic resonance imaging-visible non-viral vector for targeted neuroblastoma siRNA therapy and diagnosis.

Keywords: tumor targeting, GD2, non-viral vector, Bcl-2 small interfering RNA, magnetic resonance imaging

Introduction

Neuroblastoma (NB) is the most common extracranial solid tumor in children. It is also the most common cancer diagnosed in children less than 1 year of age.[1] Based on the International Neuroblastoma Staging System of stage, group, and tumor biology, patients can be assigned to a low-, intermediate- or high-risk group.[2] Despite advanced therapies including surgery, radiotherapy, and chemotherapy, children with high-risk NB have an extremely poor prognosis.[3] The 5-year survival rate of high-risk patients is as low as 20%–25%, and most of the patients develop metastatic dissemination.[4] Therefore, novel therapies are urgently needed.

Small interfering ribonucleic acid (siRNA) is a promising candidate for the treatment of many diseases.[5,6] The *Bcl-2* gene is a key apoptosis inhibitor that is overexpressed in many tumors. We used SignalSilence Bcl-2 siRNA (Cell Signaling Technology, Inc, Danvers, MA, USA) to specifically inhibit Bcl-2 expression and promote tumor apoptosis. However, siRNA cannot readily penetrate through cell membranes because of its highly negative charge. Therefore, effective delivery systems are needed in order to overcome this problem. The challenge remains to develop safe and efficient siRNA delivery systems for siRNA therapy. Up to now, the siRNA delivery vehicles can be classified into two categories: viral and non-viral systems.[7] Viral vectors are highly efficient delivery systems for nucleic acids, but some of their properties, including

the potential of oncogenicity, host immune responses, and the high cost of production, restrict their clinical application. These drawbacks have made non-viral vectors an alternative to viral vectors. To deliver siRNA efficiently, a large number of non-viral delivery systems and methods have been introduced, including chemical modifications of siRNA, cationic polymers, cationic lipids, cell-penetrating peptide, and targeted delivery.[8,9] Cationic polymers readily bind and condense nucleic acids, therefore, they have been commonly used as transfection vehicles for siRNA. Of the many cationic polymers, polyethylenimine (PEI) has been widely used for nucleic acid delivery. The "proton-sponge" effect of PEI allows siRNA to escape from endosomes and to deliver nucleic acids into the cell.[10] The highly branched polymers such as branch polyethylenimine (BPEI, 25 kDa), have been frequently used because they offer significantly more protection against nuclease degradation. However, the large amount of positive charge results in rather high cellular toxicity and is the major limiting factor for their application in vivo. Therefore, polyethylene glycol (PEG) was introduced to PEI (PEG-g-PEI) to reduce cytotoxicity. The incorporation of the hydrophilic polymer PEG into a polymeric gene delivery system has been proven to reduce the positive charge and therefore improve biocompatibility. PEGylation could improve the stability of polyplexes and could reduce their toxicity. Furthermore, PEGylation could also provide a frame for many modifications, such as antibodies, growth factors and peptides.[11–13]

To improve the efficiency of the siRNA delivery system, targeted siRNA delivery systems are needed. Targeted delivery systems can be recognized by specific cell receptors that mediate endocytosis. In the treatment of cancer, anticancer monoclonal antibodies targeting specific antigens on tumor cell surfaces are increasingly applied. However, clinical application of the antibody has been limited due to its immunogenicity, large size (150 kDa), and subunit structure.[14] In contrast, the single-chain antibodies may be more useful for many applications. These antibodies are constructed from a heavy chain (V_H) and a light chain (V_L) that are connected via a short peptide linker, and they retain the specificity of the original immunoglobulin; single-chain antibodies have lower molecular weights than other antibodies. Additionally, GD2 ganglioside is highly expressed on the surfaces of human neuroblastoma cells, which has made it an attractive target for tumor-specific antibody therapy.[15]

Magnetic resonance imaging (MRI) is widely used in the clinical setting because it is non-invasive, can produce high-definition images and can depict pathological tissues. Gao et al reported on the MRI-visible polymer for anti-cancer drug delivery.[16] Liao et al attached doxorubicin to targeted magnetic nanoparticles and then used MRI to perform the targeted drug delivery.[17] Inspired by these achievements, we proposed to develop a multifunctional delivery system based on PEG and PEI for the joint delivery of siRNA and superparamagnetic iron oxide nanoparticles (SPIONs). The delivery capability of this multifunctional carrier was assessed through co-delivering SPION and siRNA against the *Bcl-2* gene, which is a key apotosis inhibitor overexpressed in many malignant tumors. It is well known that SPIONs produce low signal intensities on MRI. Therefore, we constructed an MRI-visible siRNA delivery system by attaching SPIONs to PEG-g-PEI. Furthermore, a targeted magnetic nanoparticulate vector was constructed by attaching a GD2 single-chain antibody ($scAb_{GD2}$) to PEG-g-PEI-SPION ($scAb_{GD2}$-PEG-g-PEI-SPION).

Materials and method

Materials

PEG-g-PEI-SPION, a magnetic non-viral delivery vector, was synthesized by our lab as previously reported.[18] The GD2 antibody was purchased from BD Bioscience Pharmingen (San Jose, CA, USA). SK-N-SH cells from a human neuroblastoma cell line were purchased from the Institute of Biochemistry and Cell Biology (CAS, China). HepG2 cells from a human liver cancer cell line were purchased from the Institute of Biochemistry and Cell Biology (CAS, China). Dulbecco's modified Eagle's medium/F-12 (DMEM) and fetal bovine serum were purchased from Invitrogen Corporation (Carlsbad, CA, USA). The fluorescent staining agent 4′,6-diamidion-2-phenylindole (DAPI) was purchased from Roche (Roche, Germany). Alexa Fluor 488 and Alexa Fluor 555 were purchased from Molecular Probes, Inc, (Eugene, OR, USA). The Cell Counting Kit-8 (CCK-8) was purchased from Dojindo Laboratories (Kumamoto, Japan). FITC-siRNA, Bcl-2 siRNA, Rabbit anti-human Bcl-2 antibody and horseradish peroxidase (HRP)-conjugated goat anti-rabbit antibody were purchased from Cell Signaling Technology (CST, USA). Alexa Fluor 488-labeled siRNA was purchased from Sangon Biotech (Shanghai, China).

Synthesis of $scAb_{GD2}$- PEG-g-PEI-SPION

A total of 200 μL of GD2 antibody (0.5 mg/mL) was dissolved in 200 μL of ethylenediaminetetraacetic acid (EDTA) solution (0.5 M, pH = 8.0). 100 mg of 2-mercaptoethylamine and 20 μL of EDTA solution were mixed with phosphate buffered saline (PBS) (1 mL) and were then added to the

aforementioned antibody solution. After incubation at 37°C for 90 min, the resulting $scAb_{GD2}$ solution was washed three times with PBS (containing 0.5 M EDTA solution) in an Amicon cell (MWCO = 10 kDa). 200 μg of Mal-PEG-COOH dissolved in 200 μL of PBS containing 0.5 M EDTA solution was added to the $scAb_{GD2}$ solution and incubated at 4°C overnight. The solution containing $scAb_{GD2}$-functionalized PEG ($scAb_{GD2}$-PEG-COOH) was washed three times with PBS in an Amicon cell (MWCO = 10 kDa). 10 μg of both 1-ethyl-3-(3-dimethylaminepropyl) carbodiimide and N-hydroxysuccinimide were added to the purified solution and incubated at 4°C for 10 min; PEG-g-PEI-SPION (200 μg) was then added, and the solution was incubated overnight at 4°C, resulting in $scAb_{GD2}$-PEG-g-PEI-SPION as the end product.

Polyplex formation

Bcl-2 siRNA (100 nM) and the delivery vector (PEG-g-PEI-SPION, $scAb_{GD2}$-PEG-g-PEI-SPION) were mixed according to various nitrogen-phosphorus (N/P) ratios. The combination was fully mixed and then kept at room temperature for 30 min for polyplex formation.

Gel retardation assay

Agarose gel electrophoresis was performed on a Bio-Rad Sub-Cell electrophoresis cell (Bio-Rad Laboratories, Inc, USA) to assess the siRNA condensation capacity of the delivery agents, and images were captured on a DNR Bio-imaging System (DNR Bio-imaging Systems Ltd, Israel). Polyplexes (PEG-g-PEI-SPION/siRNA, $scAb_{GD2}$-PEG-g-PEI-SPION/siRNA) were formed at various N/P ratios from 1.8 to 2.4 and were mixed with 50% glycerin. They were then loaded onto the 1% agarose gels with ethidium bromide (0.1 μg/mL), which were run with Tris-acetate (TAE) buffer at 120 V for 25 min. UV light was used to reveal siRNA band shifts.

Cell viability assay

To evaluate the cytotoxicities of the PEG-g-PEI-SPION/siRNA and $scAb_{GD2}$-PEG-g-PEI-SPION/siRNA polyplexes, a CCK-8 assay was performed according to the manufacturer's protocol. Cells were seeded at a density of 5×10^3 cells per well in a 96-well plate and were cultured for 24 hours at 37°C. The cells were then incubated in 100 μL of fresh medium at various polymer (PEG-g-PEI-SPION/siRNA, $scAb_{GD2}$-PEG-g-PEI-SPION/siRNA) concentrations for 48 hours. Subsequently, 10 μL of CCK-8 solution was added to each well, and the cells were incubated for an additional 3 hours. The absorbances at 450 nm and 620 nm were recorded on a Tecan Infinite F200 Multimode plate reader (Tecan Trading AG, Switzerland). All experiments were conducted in triplicate.

Particle size and zeta potential measurements

The particle sizes were measured by dynamic light scattering. Measurements were performed at 25°C on Plus/BI-MAS equipment (Brookhaven Instruments Corporation, USA). The zeta potential of each sample was measured by a Zeta Plus Analyzer (Brookhaven Instruments Corporation, USA) to determine the electrophoretic light scattering at 25°C. The particle size and zeta potential of each sample were measured five times.

Transfection experiments

The FITC-labeled negative control siRNA (siNC-FITC) was used to evaluate transfection efficiency. Transfection experiments were performed in a 6-well plate, the applied siRNA amount per well in cell culture was set constantly to 100 nM (according to the manufacturer's protocol). SK-N-SH cells were seeded at a density of 1×10^6 cells per well prior to the transfection reaction. PEG-g-PEI-SPION/siRNA and $scAb_{GD2}$-PEG-g-PEI-SPION/siRNA polyplexes formed at various N/P ratios were added into each well. After 4 hours of incubation, the culture medium was replaced with fresh DMEM medium, and cells were incubated for an additional 8 hours. Then cells were washed with PBS (pH = 7.4), inspected under a Carl Zeiss Aviox-1 inverted fluorescence microscope, and quantitatively analyzed using a FACScan flow cytometer (Becton Dickinson, Franklin Lakes, NJ, US).

For the free ligand competitive inhibition assay, cells were pre-treated with 10 μL of free GD2 antibody for 30 min before $scAb_{GD2}$-PEG-g-PEI-SPION/siRNA was added into the culture medium.

Cell uptake of polyplexes

Multiple fluorescent labeling of polyplexes was employed for confocal laser scanning microscopy (CLSM) experiments. Alexa Fluor 555 (Life Technologies Corporation, Carlsbad, CA, USA), an amine-reactive dye, was dissolved in dimethyl sulfoxide to a final concentration of 1 mg/mL. A delivery agent, such as $scAb_{GD2}$-PEG-g-PEI-SPION, was dissolved in 1 mL of a 0.1 M sodium bicarbonate buffer (pH = 8.3–9.0). The reactive dye was slowly added under stirring. The mixture was incubated in the dark and stirred for 1 hour at room temperature. The unreacted labeling reagent was eliminated from the solution by ultrafiltration

in an Amicon cell (MWCO = 10 kDa). Using this method, the dye-delivery agent solution was washed four times with PBS (pH = 7.4) until no absorption at 555 nm was detected in the filtrate.

SK-N-SH cells were seeded at a density of 2×10^3 cells in a confocal dish. The Alexa Fluor 488-labeled siRNA (100 nM) was complexed with the appropriate amount of Alexa Fluor 555-labeled delivery agent (PEG-g-PEI-SPION, $scAb_{GD2}$-PEG-g-PEI-SPION) at an N/P ratio of 10; the components were completely mixed and were then kept at room temperature for 30 min. The prepared polyplexes were added into the DMEM cell culture medium. After 8 hours, the cells were washed three times with fresh PBS and incubated for an additional 15 min after adding the DNA-staining agent, DAPI, dissolved in ultrapure water (1 mg/mL). CLSM observations were performed using a Zeiss LSM 510 META microscope (Carl Zeiss Cl, Ltd, Gottingen, Germany). The free ligand competitive inhibition assay was also performed.

In vitro MRI scan

SK-N-SH cells were plated at a density of 1×10^6 cells per well on 6-well plates and incubated for 2 hours in the presence of PEG-g-PEI-SPION or $scAb_{GD2}$-PEG-g-PEI-SPION at Fe concentrations of 5, 10, 20, and 40 μg/mL in DMEM medium. The cells were washed three times with PBS, trypsinized, resuspended in a 4% gelatin solution, and scanned at room temperature with a 1.5T MR scanner (GE Healthcare UK Limited, Buckinghamshire, UK). A wrist coil with an inner diameter of 3 inches was used for this study. T_2-weighted images were acquired using the following parameters: repetition time/echo time 5000/100 ms; FOV, 150 mm; matrix, 256 × 256; slice thickness, 1 mm. The signal intensities of the control and treated cells were determined using a circular 30 mm^2 region of interest. The signal intensity of treated cells was normalized by comparison with that of control cells. The free ligand competitive inhibition assay was performed as usual.

Assessment of cell apoptosis

Cells were plated at a density of 1×10^4 cells per well on a 24-well plate, the applied siRNA amount per well in cell culture was set constantly to 100 nM. After incubating the cells for 48 hours, the TUNEL assay was performed using an In Situ Cell Death Detection Kit with Tetramethylrhodamine red (Roche, Mannheim, Germany) according to the manufacturer's protocol. In brief, after 300 μL of 4% paraformaldehyde in PBS (pH = 7.4) was added to each well, the cells were incubated for 20 min at room temperature and then washed three times with PBS (pH = 7.4). After 300 μL of 0.1% Triton-X100 in 0.1% sodium citrate was added to each well, the cells were incubated for 20 min at room temperature and then washed three times with PBS (pH = 7.4). Then 50 μL of TUNEL reaction mixture was added into each well, and the cells were incubated for 1 hour at 37°C in a humidified atmosphere in the dark. The cells were then washed with PBS (pH = 7.4), the DNA-staining agent DAPI dissolved in ultrapure water (1 mg/mL), was added, and the cells were incubated for an additional 15 min. The cells were directly analyzed by fluorescence microscopy. Tetramethylrhodamine red-labeled nucleotides, incorporated in nucleotide polymers, were detected under the inverted fluorescence microscope.

Reverse transcription polymerase (RT-PCR) analysis

After transfection for 48 hour, RNA was extracted using TRIzol reagent (Invitrogen, Carlsbad, CA, USA). RT-PCR was performed using the PrimeScript RT-PCR Kit (Takara, Dalian, China) according to the manufacturer's instructions. The forward and reverse primers targeting Bcl-2 sequence were 5′-TGTCCCTTTGACCTTGTTTCT-3′ and 5′-TCATTTGCCATCTGGATTTT-3′, respectively. The PCR was run on a StepOne Plus Real-time PCR System (Applied Biosystems, Foster City, CA, USA). All experiments were performed in triplicate. The PCR reaction conditions were as follows: 95°C for 10 min; and 40 cycles of 95°C/10 s, 60°C/20 s, and 72°C/20 s.

Western blot analysis

After transfection for 48 hours, total protein was extracted using ProteoJET™ Mammalian Cell Lysis Reagent (Fermentas, Canada) with Phenylmethanesulfonyl fluoride, and the protein concentrations were measured using the BCA Protein Assay Kit (CWBIO, Beijing, China). Total proteins (20 μg) were separated on 8% SDS-PAGE gels (Bio-Rad Laboratories Inc, Hercules, CA, USA) and transferred onto polyvinylidene difluoride (PVDF) membranes by electroblotting. The membranes were blocked with 5% nonfat milk in Tris-buffered saline and Tween (TBST) buffer for 1 hour at room temperature and then incubated with a rabbit anti-human Bcl-2 antibody (1:1000 dilution) at 4°C overnight. After three washes with TBST, the membranes were incubated with HRP-conjugated goat anti-rabbit antibody diluted at 1:5000 in TBST buffer for 1 hour at room temperature. Enhanced chemiluminescence detection reagents (Millipore, USA) were used, and the results were photo-documented.

In vivo studies

SK-N-SH cells (3.0×10^6 cells per mouse) were injected subcutaneously into the left thighs of 15 female nude mice (15–16 g). Three days after injection, the mice were divided into three groups (5 mice per group). Different injections were performed according to grouping: Group 1, PBS buffer; Group 2, PEG-g-PEI-SPION/siRNA; and Group 3, $scAb_{GD2}$-PEG-g-PEI-SPION/siRNA. The injections were performed daily through the tail vein for 15 days. The injection was performed everyday at a dose of 1.6 mg siRNA/Kg body weight per injection. Tumor size was measured using calipers across the longest (a) and shortest diameters (b) of the tumors, and their volumes were calculated by $V = ab^2$. Tumor volumes were measured on the last day. All animal studies were approved by the animal care and use committee at the institute.

Immunohistochemistry

Mice were sacrificed, and the tumors were removed, fixed in 4% paraformaldehyde and then embedded in paraffin. After deparaffinization and rehydration, sections were incubated with 3% hydrogen peroxide. They were then blocked with protein blocking serum for 5 min and incubated with rabbit anti-human Bcl-2 antibody (1:50 dilution) at 4°C overnight. After being washed with PBS, the sections were incubated with HRP-conjugated goat anti-rabbit antibody for 30 min and were subsequently stained with 3,3-diaminobenzidine. They were then kept in the dark at room temperature for 3 min before they were washed with PBS and stained with hematoxylin.

In vivo MRI scan

To further verify the tumor-targeting capacity of $scAb_{GD2}$-PEG-g-PEI-SPION, we performed animal studies. All animal studies were approved by the animal care and use committee at the institute. All animals were bred by professionals at Zhongshan University. SK-N-SH cells expressed GD2 at high levels, while HepG2 (human hepatic carcinoma cells) hardly expressed any GD2; therefore, we chose SK-N-SH cells as the target tumor and HepG2 as the non-target tumor. We divided 12 female nude mice (15–16 g, 4-week old BALB/c Nude mice) into two groups and injected 3.0×10^6 SK-N-SH cells or 3.0×10^6 HepG2 cells subcutaneously into their left thighs. Three days after cell implantation, the mice developed left thigh tumors that were 100–150 mm^3 in size. Six mice with SK-N-SH tumors were divided into two groups (Group 1, Group 2); 6 mice with HepG2 tumors were divided into two groups (Group 3, Group 4). They were then anesthetized with 10% chloral hydrate (5 μL/g), and MRI was performed prior to injection. MRI was repeated 5 hours after the injection of 250 μL PEG-g-PEI-SPION (0.75 μg/μL) or $scAb_{GD2}$-PEG-g-PEI-SPION (0.75 μg/μL) intravenously through the tail vein. MRI was performed with a 1.5T MRI scanner (GE Healthcare, UK) using a 5-cm linearly polarized birdcage radio frequency mouse coil. T_2-weighted images were acquired using a fast spin-echo sequence (repetition time = 2000 ms; echo time = 80 ms; FOV 3 cm × 3 cm; slice thickness 1.0 mm; flip angle 90°). The signal intensities of the tumors (before injection and after injection) were determined using a circular 30 mm^2 region of interest. The signal intensity of tumors after injection was normalized by comparison with that of tumors before injection.

Histology analysis

The mice were sacrificed after the MRI was completed. The tumors were excised, fixed in 4% paraformaldehyde and embedded in paraffin. Histological sections were prepared for analysis using Prussian blue staining.

Statistical analysis

All data were analyzed with the Statistical Package for the Social Sciences version 11.5 (SPSS Inc, Chicago, IL, USA). The results were expressed as the means ± SE, and $P < 0.05$ was considered statistically significant. All statistical tests were two-sided.

Results

Gel retardation

Agarose gel electrophoresis was performed to confirm the complexation between siRNA and PEG-g-PEI-SPION or $scAb_{GD2}$-PEG-g-PEI-SPION. The complexation of siRNA with cationic polymers is due to the electrostatic neutralization and size of the polymers, by which siRNA partially or completely loses its negative charge, resulting in the retardation of its mobility in the electric field. Therefore, the capacity of the polymer to complex siRNA could be measured by the retardation of siRNA mobility in gel electrophoresis. As shown in Figure 1, both PEG-g-PEI-SPION and $scAb_{GD2}$-PEG-g-PEI-SPION started to form complexes with siRNA at low N/P ratios, and complete retardation of siRNA migration occurred at an N/P ratio of 2.2.

Cell viability analysis

A CCK-8 assay was performed to evaluate the cytotoxicities of the polyplexes. The human neuroblastoma cell line SK-N-SH was chosen as the target because of its high GD2

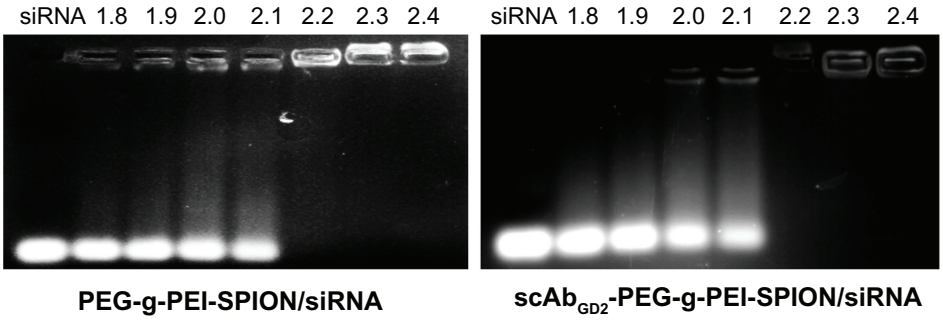

Figure 1 Gel electrophoresis of PEG-g-PEI-SPION/siRNA and scAb$_{GD2}$-PEG-g-PEI-SPION/siRNA at various N/P ratios from 1.8 to 2.4.
Notes: The band intensities of nontargeting polyplexes. The brightness of EB-stained siRNA bands decreased with increasing the N/P ratio of nontargeting and targeting polyplexes. siRNA condensation by both PEG-g-PEI-SPION and scAb$_{GD2}$-PEG-g-PEI-SPION completely retarded the siRNA motion by almost the same amount at an N/P ratio of 2.2.
Abbreviations: PEG-g-PEI-SPION, polyethylene glycol-grafted polyethylenimine superparamagnetic iron oxide nanoparticle; siRNA, small interfering ribonucleic acid; N/P, nitrogen-phosphorus; EB, ethidium bromide.

expression level. SK-N-SH cells were incubated with PEG-g-PEI-SPION/siRNA and scAb$_{GD2}$-PEG-g-PEI-SPION/siRNA for 48 hours at N/P ratios of 2.5 to 30. As shown in Figure 2, cell viability decreased gradually as N/P ratio increased. At an N/P ratio of 10, the cell viabilities of PEG-g-PEI-SPION/siRNA and scAb$_{GD2}$-PEG-g-PEI-SPION/siRNA were 96.45% ± 1.31% and 95.47% ± 1.03%, respectively. There were no significant differences between the two groups at the different N/P ratios ($P > 0.05$), which illustrated that the connection of scAb$_{GD2}$ did not increase the cytotoxicity of PEG-g-PEI-SPION.

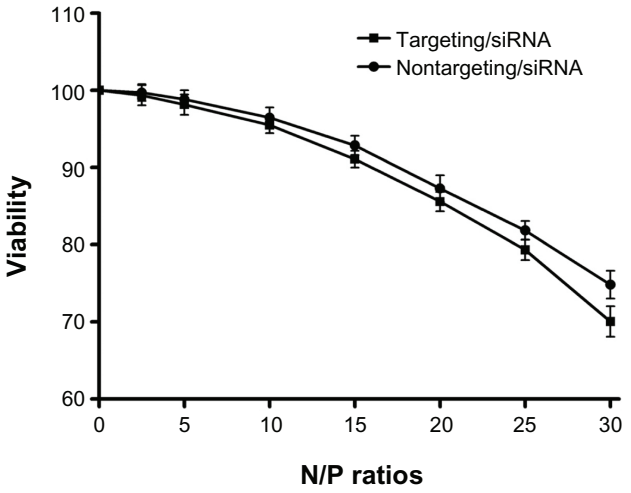

Figure 2 The cytotoxicities of PEG-g-PEI-SPION/siRNA and scAb$_{GD2}$-PEG-g-PEI-SPION/siRNA polyplexes in SK-N-SH cells.
Notes: The cytotoxicities of PEG-g-PEI-SPION/siRNA and scAb$_{GD2}$-PEG-g-PEI-SPION/siRNA polyplexes in SK-N-SH cells were evaluated using the CCK-8 assay. The siRNA concentration was 0.15 μg per well (in 300 μL cell culture medium), and the polyplex added into each well was adjusted according to the N/P ratios. There were no statistical differences between the two groups ($P > 0.05$). The results were expressed as the means ± SD (n = 3).
Abbreviations: PEG-g-PEI-SPION, polyethylene glycol-grafted polyethylenimine superparamagnetic iron oxide nanoparticle; siRNA, small interfering ribonucleic acid; CCK-8, cell counting kit-8; N/P, nitrogen-phosphorus; P, probability level; SD, standard deviation.

Particle size and zeta potential

The particle size and zeta potential of nontargeting and targeting complexes varied with various N/P ratios. The particle size decreased with increasing N/P ratio of nontargeting and targeting polyplexes, maintained around 90 nm and 96 nm, respectively, when the N/P ratio reached around 10. On the contrary, the zeta potential increased with increasing the N/P ratio (Figure 3). On the whole, the particle size decreased, whereas the zeta potential of polyplexes increased with increasing N/P ratio.

siRNA transfection in vitro

After SK-N-SH cells were incubated with PEG-g-PEI-SPION/siRNA (targeting), scAb$_{GD2}$-PEG-g-PEI-SPION/siRNA (nontargeting) and scAb$_{GD2}$-PEG-g-PEI-SPION/siRNA with free GD2 antibody (targeting/GD2) at various N/P ratios, the siRNA transfection efficiency was assessed. Targeting polyplexes exhibited much stronger green fluorescence than nontargeting polyplexes and targeting/GD2. As shown in Figure 4, quantitative flow cytometric analysis indicated that at the same N/P ratio, the transfection efficiency of targeting polyplexes was clearly higher than those of nontargeting polyplexes and targeting/GD2 ($P < 0.01$). The transfection efficiency of targeting polyplexes reached the highest value (56.34% ± 2.13%) at N/P 10, while nontargeting polyplexes and targeting/GD2 reached their highest transfection efficiencies at 13.45% ± 1.98% and 15.67% ± 2.56%, respectively, at an N/P ratio of 10.

Cellular uptake and distribution of polyplexes

We used CLSM to investigate the uptake of polyplexes by SK-N-SH cells after 2 hours of incubation. To obtain better visualization of the intracellular distribution of polyplexes, the nuclei

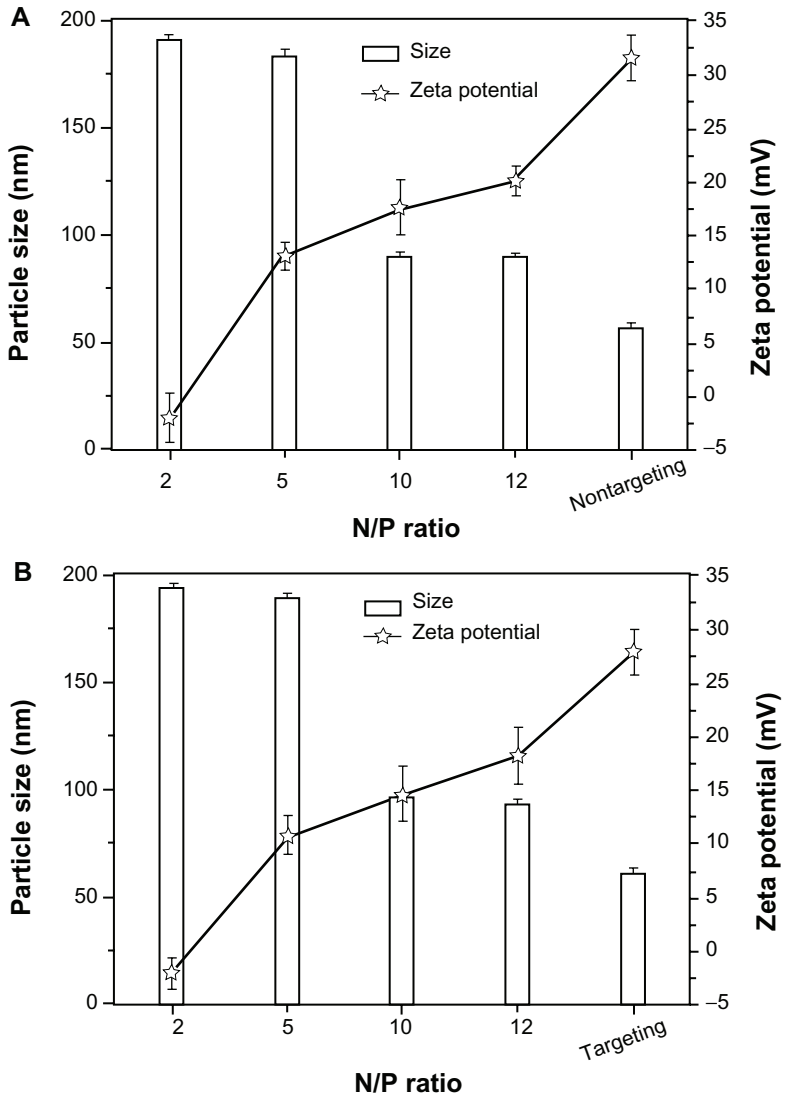

Figure 3 The particle size and zeta potential of PEG-g-PEI-SPION (nontargeting), $scAb_{GD2}$-PEG-g-PEI-SPION (targeting), PEG-g-PEI-SPION/siRNA and $scAb_{GD2}$-PEG-g-PEI-SPION/siRNA polyplexes.

Abbreviations: PEG-g-PEI-SPION, polyethylene glycol-grafted polyethylenimine superparamagnetic iron oxide nanoparticle; siRNA, small interfering ribonucleic acid; N/P, nitrogen-phosphorus.

were stained blue with DAPI. Alexa Fluor 488-labeled siRNA was used to visualize the cellular uptake of siRNA. Alexa Fluor 555-labeled polymer was used to visualize the cellular uptake of the polymer. As shown in Figure 5, cells incubated for 2 hours with $scAb_{GD2}$-PEG-g-PEI-SPION/siRNA (targeting) displayed clearly stronger agent (red) and siRNA (green) fluorescence compared to cells incubated with PEG-g-PEI-SPION/siRNA (nontargeting). Moreover, SK-N-SH cells incubated with free GD2 antibody significantly inhibited the uptake of targeting polyplexes into the cells. These results demonstrated that endocytosis of $scAb_{GD2}$-PEG-g-PEI-SPION/siRNA was mediated by the specific interaction between the $scAb_{GD2}$ and GD2 receptors; consequently, polyplexes with $scAb_{GD2}$ can significantly enhance the cellular uptake of SK-N-SH cells.

In vitro MRI scan

As shown in Figure 6, with increasing Fe concentrations in the polymer, the MRI signal intensity of SK-N-SH cells decreased. There was a significant decrease in MRI signal intensity when the Fe concentration of the polymer was higher. At the same Fe concentration, cells incubated with targeting polymer exhibited a significant decrease compared to when they were incubated with nontargeting and targeting/GD2 polymers.

Effects of Bcl-2 siRNA on cell apoptosis

To further verify the effects of Bcl-2 siRNA, TUNEL analysis was conducted to quantify cell apoptosis. TUNEL was conducted, and the numbers of TUNEL-positive cells (ie, cells

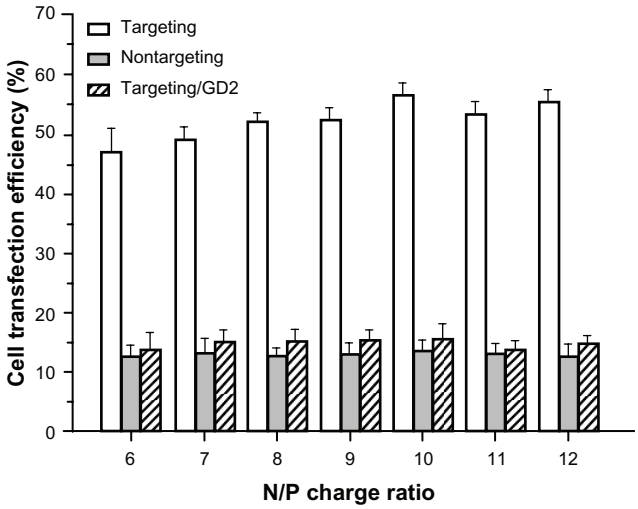

Figure 4 The transfection efficiency in SK-N-SH cells.
Notes: The transfection efficiency in SK-N-SH cells at various N/P ratios of PEG-g-PEI-SPION/siRNA (nontargeting), $scAb_{GD2}$-PEG-g-PEI-SPION/siRNA (targeting) and $scAb_{GD2}$-PEG-g-PEI-SPION/siRNA with free GD2 antibody (targeting/GD2). There were significant differences between targeting and nontargeting polyplexes.
Abbreviations: PEG-g-PEI-SPION, polyethylene glycol-grafted polyethylenimine superparamagnetic iron oxide nanoparticle; siRNA, small interfering ribonucleic acid; N/P, nitrogen-phosphorus.

with red fluorescence) were counted to obtain the percentage of apoptotic cells. As shown in Figure 7A, nuclei in apoptotic cells displayed strong red fluorescence due to the existence of fragmented DNA. Nuclei in normal cells that were not undergoing apoptosis did not display red fluorescence. SK-N-SH cells incubated with various polyplexes exhibited significantly different levels of apoptosis. Clearly, $scAb_{GD2}$-PEG-g-PEI-SPION/siRNA (targeting) treatment resulted in the highest level of cell apoptosis (50.76% ± 2.34%) among all the tested cell groups, as shown in Figure 7B. Cells incubated with nontargeting and targeting/GD2 resulted in 10.39% ± 1.76% and 11.34% ± 2.26% cell apoptosis, respectively, which are significantly lower than the level induced by the targeting polyplexes.

Suppression on *Bcl-2* gene expression

After 48 hours of cell transfection, *Bcl-2* gene expression in SK-N-SH cells was evaluated at both the mRNA and protein levels. RT-PCR analysis (shown in Figure 8A) revealed that $scAb_{GD2}$-PEG-g-PEI-SPION/siRNA (targeting), PEG-g-PEI-SPION/siRNA (nontargeting), and $scAb_{GD2}$-PEG-g-PEI-SPION/siRNA with free GD2 antibody (targeting/GD2) suppressed the expression of *Bcl-2* gene to 46.34% ± 1.87%, 90.21% ± 2.09%, 88.34% ± 2.45%, respectively (relative to the blank control). There were significant differences in the suppression of the *Bcl-2* gene between targeting polyplexes and nontargeting or targeting/GD2 polyplexes. Western blot analysis was then performed to evaluate the suppression of the *Bcl-2* gene at the protein level. As shown in Figure 8B, cells incubated with targeting polyplexes had significantly lower levels of Bcl-2 protein expression than cells incubated

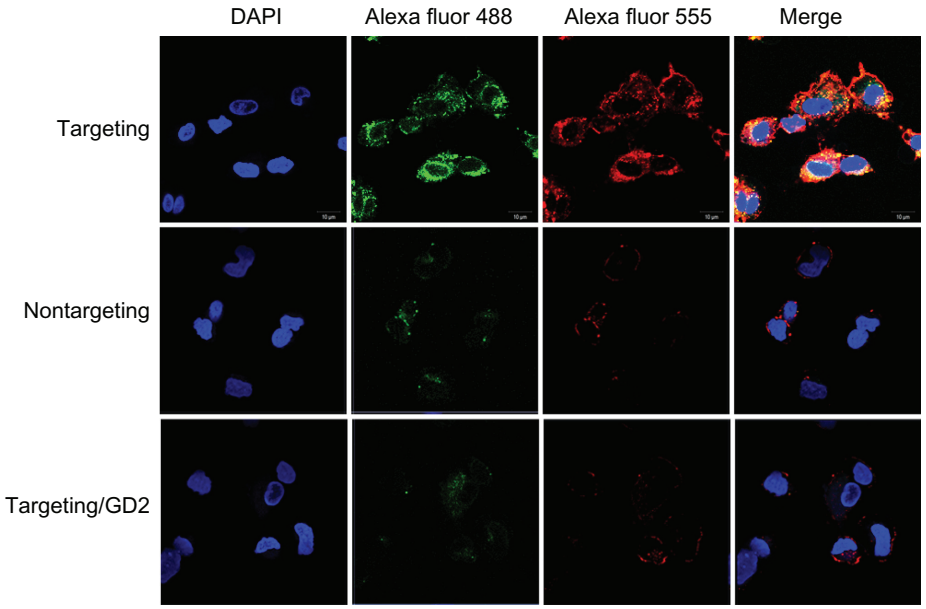

Figure 5 High magnification (100×) laser confocal microscopic images of SK-N-SH cells incubated for 2 hours with $scAb_{GD2}$-PEG-g-PEI-SPION/siRNA (targeting) and PEG-g-PEI-SPION/siRNA (nontargeting).
Notes: SK-N-SH cells were incubated for 30 minutes with free GD2 antibody and then incubated with $scAb_{GD2}$-PEG-g-PEI-SPION/siRNA (targeting/GD2) for 2 hours in cell culture medium. All polyplexes were formed at N/P = 10.
Abbreviations: PEG-g-PEI-SPION, polyethylene glycol-grafted polyethylenimine superparamagnetic iron oxide nanoparticle; siRNA, small interfering ribonucleic acid; N/P, nitrogen-phosphorus.

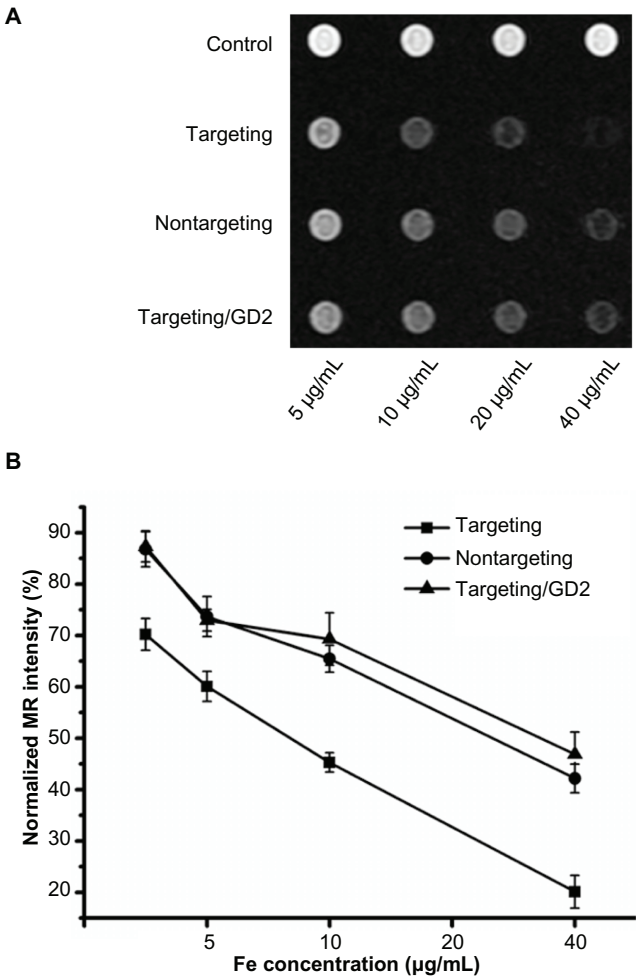

Figure 6 T_2-weighted imaging of SK-N-SH cells. (**A**) T_2-weighted imaging of SK-N-SH cells after 2-hour incubations with $scAb_{GD2}$-PEG-g-PEI-SPION, PEG-g-PEI-SPION, and $scAb_{GD2}$-PEG-g-PEI-SPION/GD2 at Fe concentrations of 5, 10, 20 and 40 μg/mL in DMEM. Untreated cells were used as the control group. Cells were scanned with a 1.5T MRI scanner. (**B**) shows the normalized MR intensity of different polymers at various Fe concentrations (n = 3).

Abbreviations: PEG-g-PEI-SPION, polyethylene glycol-grafted polyethylenimine superparamagnetic iron oxide nanoparticle; DMEM, Dulbecco's modified eagle medium; MRI, magnetic resonance imaging; MR, magnetic resonance.

with either nontargeting or targeting/GD2 polyplexes. The results are consistent with results obtained through RT-PCR and indicate that targeting polyplexes have a stronger suppressive effect on the *Bcl-2* gene.

Effect of targeting therapy with Bcl-2 siRNA on SK-N-SH tumors in vivo

Fifteen days after injection, the average tumor sizes were 250.34 ± 8.45 mm^3 for the PBS-control group and 123.45 ± 6.79 mm^3 for the targeting therapy group ($scAb_{GD2}$-PEG-g-PEI-SPION/siRNA). In the nontargeting therapy group (PEG-g-PEI-SPION/siRNA), the average tumor size was 234.45 ± 6.78 mm^3 (Figure 9). These results indicate that targeting therapy could significantly inhibit the development of SK-N-SH tumors when compared to the control or nontargeting therapy groups ($P < 0.01$).

Immunohistochemistry was performed to confirm the expression of the Bcl-2 protein in tumors. Cell nuclei were stained blue and the brown stains indicated the Bcl-2 protein expressed in the tumor tissue. Compared to the basal expression of Bcl-2 proteins in the tumor tissue from mice receiving PBS (Figure 10B), mice receiving targeting therapy exhibited a significant suppression in Bcl-2 expression (Figure 10F); mice receiving nontargeting therapy showed a medium level suppression in Bcl-2 expression (Figure 10D). The results demonstrated that the targeting polyplexes delivered Bcl-2 siRNA into the tumor cells more effectively than the nontargeting polyplexes.

In vivo MRI scan

To further validate the tumor-targeting capacity of $scAb_{GD2}$-PEG-g-PEI-SPION in vivo, 12 mice with one of two types of tumors (SK-N-SH, HepG2) were injected with nontargeting or targeting polymers. Prior to injection, both tumors marked with blue arrows (Figure 11A) exhibited high signal intensities on T_2-weighted MRI images. Five hours after injection of PEG-g-PEI-SPION, both SK-N-SH tumors (Group 1) and HepG2 tumors (Group 3) showed slightly low signal intensity on T_2-weighted images (marked with yellow arrows). However, five hours after injection of $scAb_{GD2}$-PEG-g-PEI-SPION, SK-N-SH tumors (Group 2) showed significant hypointense signals (marked with red arrow), while HepG2 (Group 4) showed slightly lower signal intensity on T_2-weighted images. We measured the MRI T_2-weighted signal intensity of tumors after injection with PEG-g-PEI-SPION or $scAb_{GD2}$-PEG-g-PEI-SPION (Figure 11B). The MRI intensity of tumors (before injection) defined as 100 were used as a control. The MRI T_2-weighted signal intensity of Group 1, 2, 3, and 4 decreased after injection. However, the MRI signal intensity decreased nearly 50% in Group 2. The above results demonstrated that $scAb_{GD2}$-PEG-g-PEI-SPION had tumor-targeting capacity.

Prussian blue staining was performed to further verify the existence of the targeting vectors in SK-N-SH tumors. As shown in Figure 12, many scattered blue spots were detected in SK-N-SH tumors after injection of the targeting polyplexes (Group 2). Meanwhile, few blue spots were detected in Groups 1, 3, and 4.

Discussion

RNA interference has been regarded as a useful tool for successfully silencing genes using small interfering RNA (siRNA).

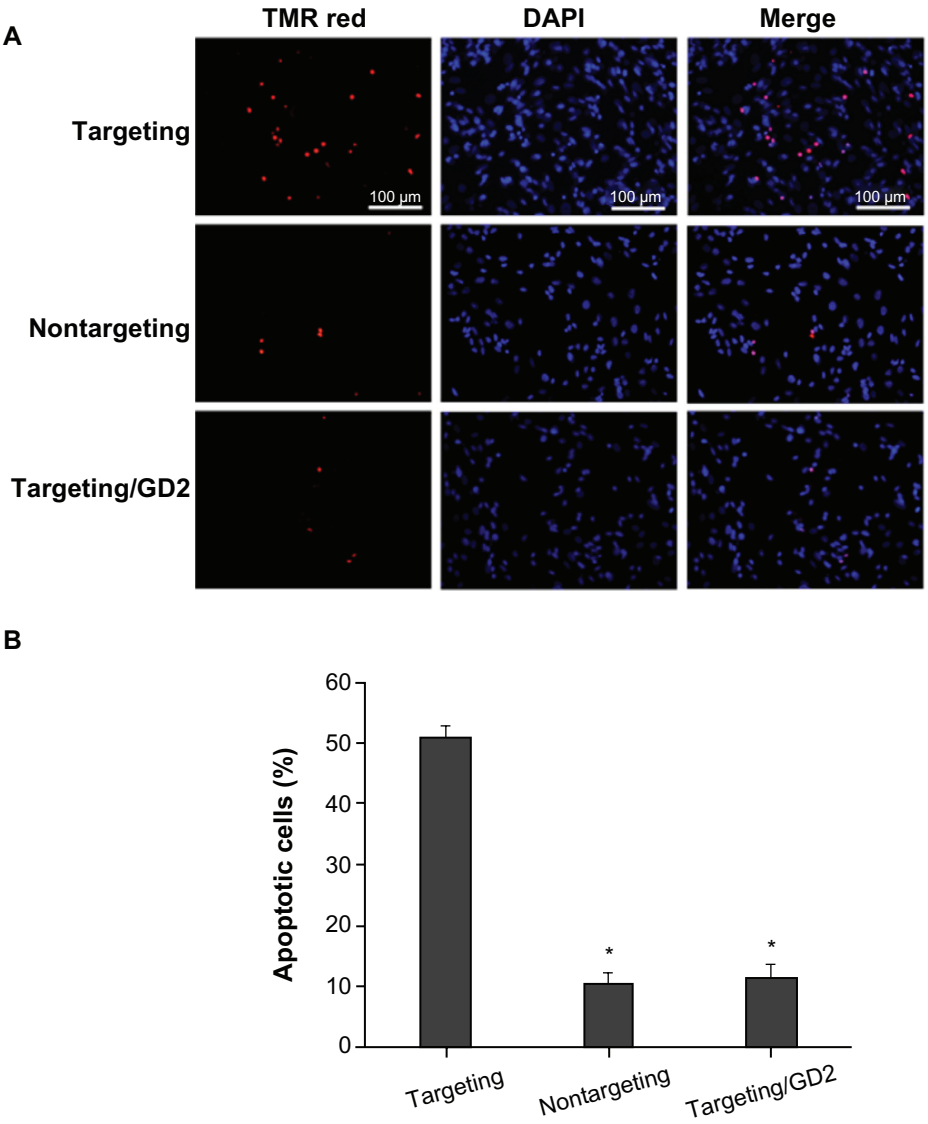

Figure 7 Cell apoptosis assessed by TUNEL at N/P = 10, the applied siRNA amount per well in cell culture was set constantly to 100 nM. (**A**) Images show cells incubated with: $scAb_{GD2}$-PEG-g-PEI-SPION/siRNA (targeting), PEG-g-PEI-SPION/siRNA (nontargeting), $scAb_{GD2}$-PEG-g-PEI-SPION/siRNA with free GD2 antibody (targeting/GD2). (**B**) Quantitative analysis of the percentage of apoptotic cells using a standard cell counting method in TUNEL assay (n = 3). When compared to $scAb_{GD2}$-PEG-g-PEI-SPION/siRNA (targeting), $^*P < 0.01$ for both nontargeting and targeting/GD2 polyplexes.

Abbreviations: siRNA, small interfering ribonucleic acid; PEG-g-PEI-SPION, polyethylene glycol-grafted polyethylenimine superparamagnetic iron oxide nanoparticle; *P*, probability level.

After uptake by cells, siRNAs are delivered into the endoribonuclease-containing complexes, which are known as RNA-induced silencing complexes. The siRNA leads the RNA-induced silencing complexes to complementary RNA molecules, and the target RNA is then cleaved and destroyed.[19] Gene silencing using siRNA is effective and specific to the target gene. This method has many potential applications in cancer treatment.[20] The *Bcl-2* gene is a critical component in the regulation of apoptosis. Overexpression of Bcl-2 is often observed in cancer cells. It prevents apoptosis of cancer cells, and it has frequently been reported that the overexpression of Bcl-2 inhibits apoptosis induced by chemotherapy.[21] Therefore, the downregulation of Bcl-2 to recover a critical apoptotic pathway in cancer cells is an important strategy. Bcl-2 is a therapeutic target in cancer cells. In our study, we used Bcl-2 siRNA to downregulate the expression of the *Bcl-2* gene in SK-N-SH cells. However, siRNA has a short half-life due to its rapid degradation in cellular cytoplasm and plasma, which is a limitation for its broader application.[22] For this reason, effective siRNA delivery systems are urgently needed. Viral and non-viral vectors have been used for siRNA delivery. Non-viral vectors are generally considered to be safer than viral vectors, and a large number of non-viral vectors have been introduced to deliver siRNAs.[23] PEI is a cationic polymer that

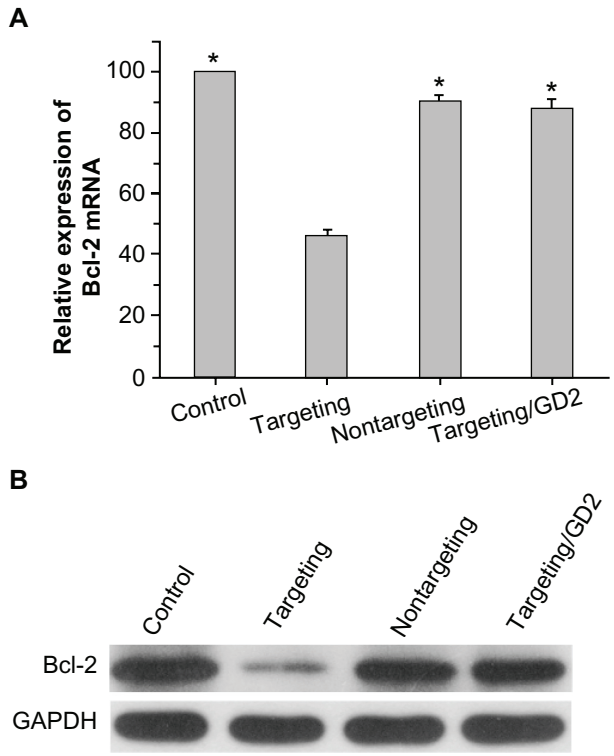

Figure 8 Efficiencies of PEG-g-PEI-SPION/siRNA, $scAb_{GD2}$-PEG-g-PEI-SPION/siRNA, and $scAb_{GD2}$-PEG-g-PEI-SPION/siRNA with free GD2 antibody in suppressing *Bcl-2* gene expression in SK-N-SH cells (N/P = 10). (**A**) Suppression of Bcl-2 mRNA levels as quantified by real-time RT-PCR (n = 3), When compared to $scAb_{GD2}$-PEG-g-PEI-SPION/siRNA (targeting), $^*P < 0.01$ for control, nontargeting and targeting/GD2 polyplexes. (**B**) Suppression of the protein expression of the *Bcl-2* gene was evaluated by Western blot analysis.

Abbreviations: PEG-g-PEI-SPION, polyethylene glycol-grafted polyethylenimine superparamagnetic iron oxide nanoparticle; siRNA, small interfering ribonucleic acid; RT-PCR, reverse transcription polymerase chain reaction; *P*, probability level.

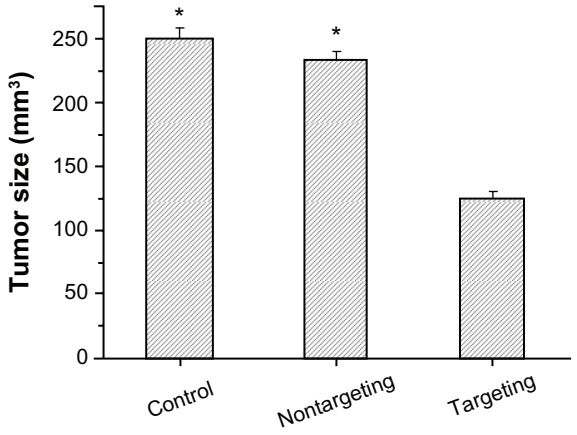

Figure 9 The average tumor size in different groups.

Notes: They include the PBS (control), PEG-g-PEI-SPION/siRNA (nontargeting), $scAb_{GD2}$-PEG-g-PEI-SPION/siRNA (targeting). When compared to $scAb_{GD2}$-PEG-g-PEI-SPION/siRNA (targeting). $^*P < 0.01$ for both control and nontargeting polyplexes. All polyplexes were formed at N/P = 10.

Abbreviations: PBS, phosphate buffered saline; PEG-g-PEI-SPION, polyethylene glycol-grafted polyethylenimine superparamagnetic iron oxide nanoparticle; siRNA, small interfering ribonucleic acid; *P*, probability level; N/P, nitrogen-phosphorus.

has been widely used as a carrier for the delivery of siRNA into cells; however, PEI has been found to be cytotoxic due to its electrostatic interactions with negatively charged cell membranes.[24,25] Therefore, PEI needs to be modified to reduce its cytotoxicity. PEG modification could reduce the positive charge of polyplexes and could thus reduce their cytotoxicity. Furthermore, PEGylation provides a frame for other modifications, such as SPION.[26] Many studies have reported that the use of PEG-PEI copolymers generally reduces the efficiency of gene delivery; therefore, it is important to introduce a targeting ligand into the gene delivery.

In this study, we combined $scAb_{GD2}$ with PEG-g-PEI-SPION to construct an MRI-visible targeted siRNA delivery vector to improve the siRNA delivery efficiency of PEG-PEI. This non-viral vector exhibited excellent binding capacity for siRNA and low cytotoxicity.

A gel retardation assay demonstrated that increasing N/P ratios resulted in improved siRNA complexation (ie, both PEG-g-PEI-SPION/siRNA and $scAb_{GD2}$-PEG-g-PEI-SPION/siRNA were completely complexed at N/P ratios above 2.2). Although a higher N/P ratio leads to better siRNA condensation, higher cytotoxicity will damage cancer cells due to electrostatic interaction. The CCK-8 assay showed that cytotoxicity increased along with higher N/P ratios. At an N/P ratio of 20, the cell viability for both groups was still over 85%. There were no statistical differences between the two groups at different N/P ratios, revealing that $scAb_{GD2}$ had no obvious cytotoxicity to SK-N-SH cells.

The tumor-targeting capacity of $scAb_{GD2}$-PEG-g-PEI-SPION in vitro was demonstrated by flow cytometric analysis and CLSM. In SK-N-SH cells, higher transfection efficiency was reached with $scAb_{GD2}$-PEG-g-PEI-SPION than with PEG-g-PEI-SPION. At an N/P ratio of 10, $scAb_{GD2}$-PEG-g-PEI-SPION/siRNA reached its highest transfection efficiency (56.34% ± 2.13%), while PEG-g-PEI-SPION/siRNA reached its highest transfection efficiency (13.45% ± 1.98%). In the free ligand competitive inhibition assay, cells were pretreated with 10 μL of free GD2 antibody for 30 min before $scAb_{GD2}$-PEG-g-PEI-SPION/siRNA was added to the culture medium. The GD2 antigen-binding site of SK-N-SH cells was saturated, and they finally reached their highest transfection efficiency of 15.67% ± 2.56%. Our results strongly suggested that the enhanced transfection efficiency of $scAb_{GD2}$-PEG-g-PEI-SPION/siRNA in SK-N-SH cells was due to the $scAb_{GD2}$-GD2-mediated cellular uptake. For better visualization of the uptake of polyplexes, multiple fluorescent labels were used. Compared to nontargeting polyplex, the targeting polyplex $scAb_{GD2}$-PEG-g-PEI-SPION/siRNA was

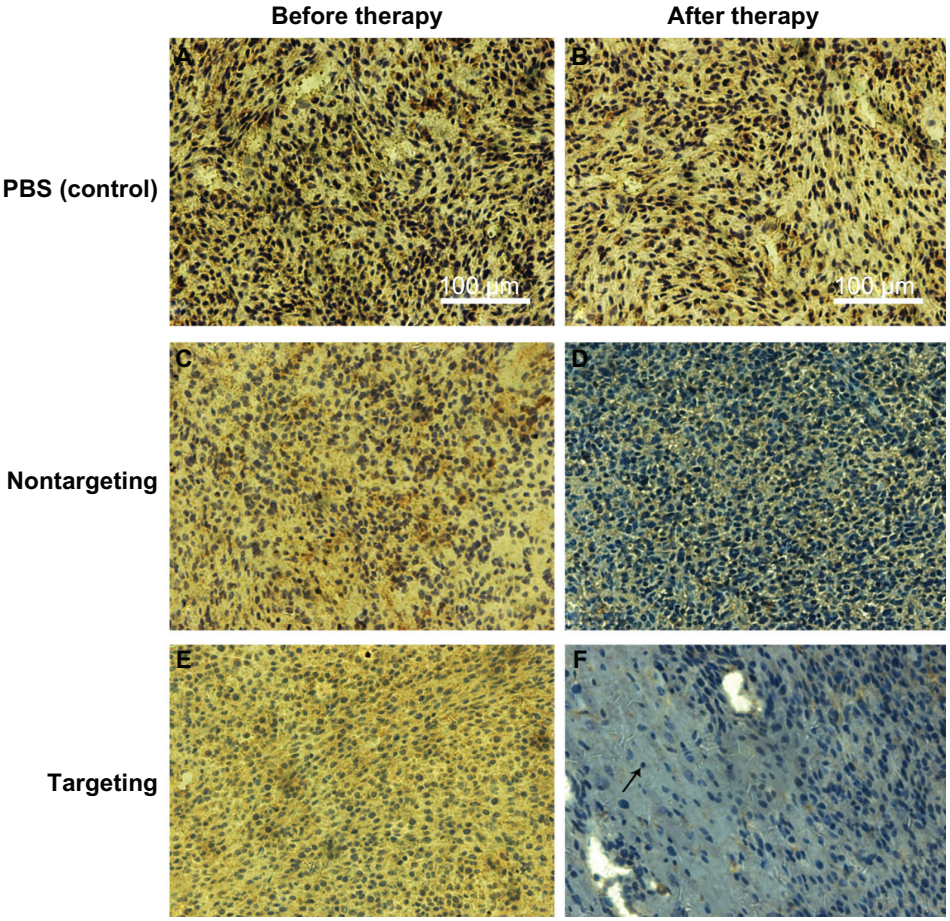

Figure 10 Immunohistological characteristics of SK-N-SH tumors (sections were immunostained with Bcl-2 monoclonal antibodies). The brown stains indicated Bcl-2 protein. (**A** and **B**) PBS control, (**C** and **D**) nontargeting polyplex therapy, (**E** and **F**) targeting polyplex therapy. The black arrow mark apoptotic cell with condensation or nuclei fragmentation.
Abbreviation: PBS, phosphate buffered saline.

efficiently taken up by cells, leading to strong green and red fluorescence. Cells pretreated with free GD2 antibody only displayed less green and red fluorescence. This assay verified that $scAb_{GD2}$ could enhance the endocytosis of the SK-N-SH cells.

After Bcl-2 siRNA was efficiently delivered into SK-N-SH cells, we tested whether increasing the expression of Bcl-2 siRNA would promote apoptosis of tumor cells in vitro and in vivo. The TUNEL assay clearly demonstrated that incubation of SK-N-SH cells with targeting polyplex resulted in apoptosis in 50.76% of the cells. RT-PCR assay revealed that the cells treated with targeting polyplex caused a 46.34% reduction of the Bcl-2 mRNA expression level, and this result was confirmed by Western blot. In vivo studies have demonstrated a significant delay in human tumor growth with the targeting polyplex therapy, indicating that Bcl-2 siRNA can promote tumor apoptosis; this result was confirmed with immunohistochemistry. The above results illustrated that Bcl-2 siRNA promotes cell apoptosis effectively and that the targeting polymer delivers siRNA effectively.

MRI has an excellent sensitivity and spatial resolution and can be used to detect the targeting capacity and MRI-visibility of $scAb_{GD2}$-PEG-g-PEI-SPION in vivo and in vitro. SK-N-SH cells were incubated with targeting, nontargeting and targeting GD2 polymers. The decrease in signal intensity of the targeting polymer was greater than that of the nontargeting or targeting GD2 polymer. After injection of the targeting polymer, SK-N-SH tumors showed a significant decrease in signal intensity in vivo, while HepG2 tumors just showed slightly low signal. The consistent results were observed in Prussian blue staining. Our results indicated that the enhanced endocytosis of the targeting polymer was due to the $scAb_{GD2}$ conjugation to PEG-g-PEI-SPION.

In summary, we constructed an MRI-visible non-viral Bcl-2 siRNA delivery vector bearing GD2 single-chain antibody ($scAb_{GD2}$) as a targeting ligand to NB cells.

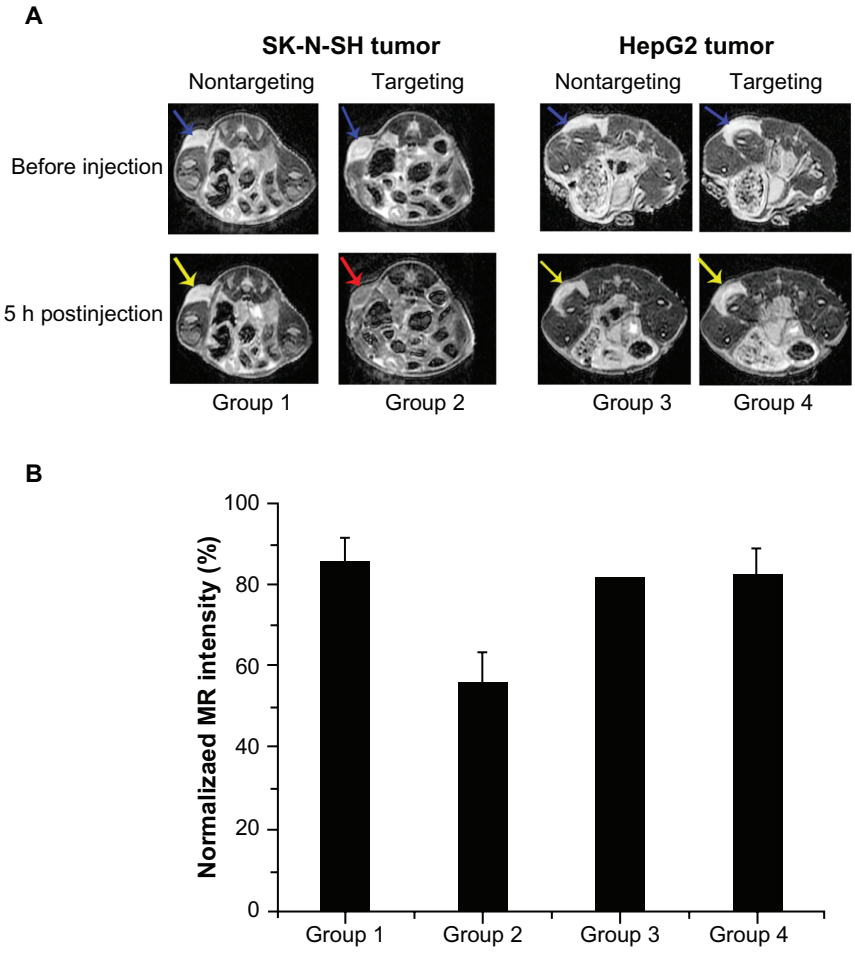

Figure 11 Tumor targeting evaluation in vivo. (**A**) Group 1: mice with SK-N-SH tumors after injection of PEG-g-PEI-SPION; Group 2: mice with SK-N-SH tumors after injection of $scAb_{GD2}$-PEG-g-PEI-SPION; Group 3: mice with HepG2 tumors after injection of PEG-g-PEI-SPION; Group 4: mice with HepG2 tumors after injection of $scAb_{GD2}$-PEG-g-PEI-SPION. (**B**) The normalized MR intensity of all groups after injection.
Abbreviations: MR, magnetic resonance; PEG-g-PEI-SPION, polyethylene glycol-grafted polyethylenimine superparamagnetic iron oxide nanoparticle.

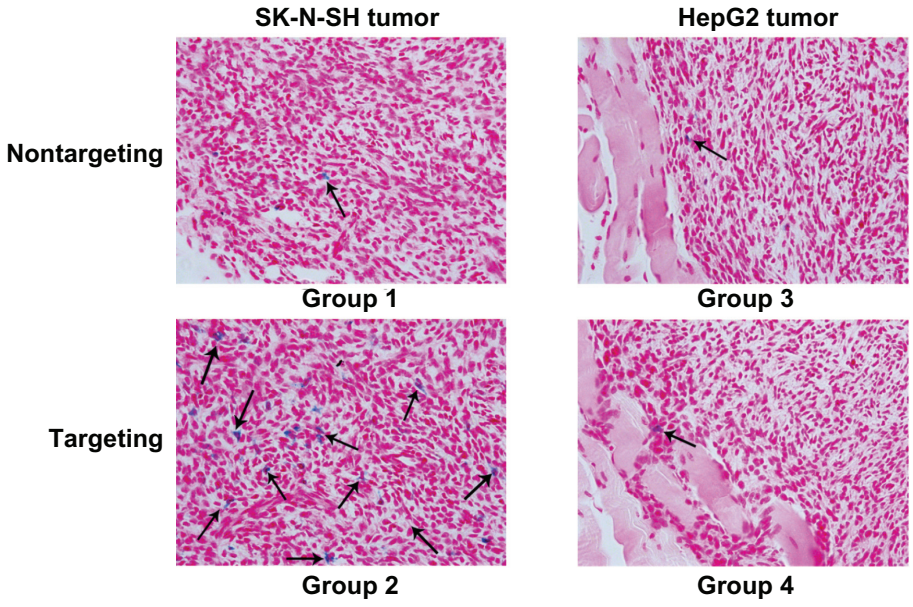

Figure 12 Prussian blue staining was performed on histological sections of tumors.
Note: Blue positive particles marked by black arrows.

This non-viral vector transferred Bcl-2 siRNA in vitro effectively and specifically promoted the apoptosis of tumor cells. The in vivo and in vitro tumor targeting capacity of the vector was verified by MRI. Our study demonstrated the potential of this vector as an MRI-visible and NB-cell-targeting siRNA carrier for NB tumor therapy.

Acknowledgments

This work was supported by the National Natural Science Foundation of China (Grant No. 81071206). NSFC-Guangdong Joint Foundation Key Project (Grant No U1032002). 2010–2012 Clinical Key Program of Ministry of Public Health of China (Grant No 164). China postdoctoral science foundation (Grant No 20100470962). National Natural Science Foundation of China (Grant No 81070349). Science and Technology Planning Project of Guangdong Province, China (Grant No 2009B030801135).

Disclosure

The authors report no conflict of interest in this work.

References

1. Maris JM, Hogarty MD, Bagatell R, Cohn SL. Neuroblastoma. *Lancet*. 2007;369(9579):2106–2120.
2. Haase GM, Perez C, Atkinson JB. Current aspects of biology, risk assessment, and treatment of neuroblastoma. *Semin Surg Oncol*. 1999;16(2):91–104.
3. Laverdiere C, Cheung NK, Kushner BH, et al. Long-term complications in survivors of advanced stage neuroblastoma. *Pediatr Blood Cancer*. 2005;45(3):324–332.
4. Tonini GP, Pistoia V. Molecularly guided therapy of neuroblastoma: a review of different approaches. *Curr Pharm Design*. 2006;12(18):2303–2317.
5. Woodrow KA, Cu Y, Booth CJ, Saucier-Sawyer JK, Wood MJ, Saltzman WM. Intravaginal gene silencing using biodegradable polymer nanoparticles densely loaded with small-interfering RNA. *Nat Mater*. 2009;8(6):526–533.
6. Davis ME, Zuckerman JE, Choi CHJ, et al. Evidence of RNA in humans from systemically administered siRNA via targeted nanoparticles. *Nature*. 2010;464(7291):1067–1070.
7. El-Aneed A. An overview of current delivery systems in cancer gene therapy. *J Control Release*. 2004;94(1):1–14.
8. Corey DR. Chemical modification: the key to clinical application of RNA interference? *J Clin Invest*. 2007;117(12):3615–3622.
9. Urban-Klein B, Werth S, Abuharbeid S, Czubayko F, Aigner A. RNA-mediator gene-targeting through systemic application of polyethylenimine (PEI)-complexed siRNA in vivo. *Gene Ther*. 2005;12(5):461–466.
10. Boussif O, Lezoualc'h F, Zanta MA, et al. A versatile vector for gene and oligonucleotide transfer into cells in culture and in vivo: polyethylenimine. *Proc Natl Acad Sci*. 1995;4(16):7297–7301.
11. Oqris M, Brunner S, R Schuller S, Kircheis R, Wagner E. PEGylated DNA/transferrin-PEI complexes: reduced interaction with blood components, extended circulation in blood and potential for systemic gene delivery. *Gene Ther*. 1999;6(4):595–605.
12. Zalipsky S. Functionalized poly(ethylene glycol) for preparation of biologically relevant conjugates. *Bioconjug Chem*. 1995;6(2):150–165.
13. Buschle M, Cotten M, Kirlappos H, et al. Receptor-mediated gene transfer into human T lymphocytes via binding of DNA/CD3 antibody particles to the CD3 T cell receptor complex. *Hum Gene Ther*. 1995;6(6):753–761.
14. Huston JS, Levinson D, Mudgett-Hunter M, et al. Protein engineering of antibody binding sites: recovery of specific activity in an anti-digoxin single chain Fv analogue produced in Escherichia coli. *Proc Natl Acad Sci*. 1988;85(16):5879–5883.
15. Navid F, Santana VM, Barfield RC. Anti-GD2 antibody therapy for GD2-expressing tumors. *Curr Cancer Drug Targets*. 2010;10(2):200–209.
16. Nasongkla N, Bey E, Ren J, et al. Multifunctional polymeric micelles as cancer-targeted, MRI-ultrasensitive drug delivery systems. *Nano Lett*. 2006;6(11):2427–2430.
17. Liao C, Sun Q, Liang B, Shen J, Shuai X. Targeting EGFR-overexpressing tumor cells using Cetuximab-immunomicelles loaded with doxorubicin and superparamagnetic iron oxide. *Eur J Radiol*. 2011;80(3):699–705.
18. Chen G, Chen W, Wu Z, et al. MRI-visible polymeric vector bearing CD3 single chain antibody for gene delivery to T cells for immunosuppression. *Biomaterials*. 2009;30(10):1962–1970.
19. Elbashir SM, Harborth J, Lendeckel W, Yalcin A, Weber K, Tuschl T. Duplexes of 21-nucleotide RNAs mediate RNA interference in cultured mammalian cells. *Nature*. 2001;411(6836):494–498.
20. Devi GR. siRNA-based approaches in cancer therapy. *Cancer Gene Ther*. 2006;13(9):819–829.
21. Jaqani HV, Josyula VR, Hariharapura RC, Palanimuthu VR, Gang SS. Nanoformulation of siRNA silencing Bcl-2 gene and its implication in cancer therapy. *Arzneimittelforschung*. 2011;61(10):577–586.
22. Patil Y, Panyam J. Polymeric nanoparticles for siRNA delivery and gene silencing. *Int J Pharm*. 2009;367(1–2):195–203.
23. Aigner A. Nonviral in vivo delivery of therapeutic small interfering RNAs. *Curr Opin Mol Ther*. 2007;9(4):345–352.
24. Fischer D, Bieber T, Li Y, Elsasser HP, Kissel T. A novel non-viral vector for DNA delivery based on low molecular weight, branched polyethyleneimine: effect of molecular weight on transfection efficiency and cytotoxicity. *Pharm Res*. 1999;16(8):1273–1279.
25. Fischer D, von Harpe A, Kunath K, Petersen H, Li Y, Kissel T. Copolymers of ethylene imine and N-(2-hydroxyethyl)-ethylene imine as tools to study effects of polymer structure on physicochemical and biological properties of DNA complexes. *Bioconjug Chem*. 2002;13(5):1124–1133.
26. Zalipsky S. Functionalized poly(ethylene glycol) for preparation of biologically relevant conjugates. *Bioconjug Chem*. 1995;6(2):150–165.